Atomistic mechanisms for wurtzite-to-rocksalt structural transformation in cadmium selenide under pressure

Fuyuki Shimojo,[1,2] Sanjay Kodiyalam,[1,3] Ingvar Ebbsjö,[4] Rajiv K. Kalia,[1] Aiichiro Nakano,[1] and Priya Vashishta[1]

[1]*Collaboratory for Advanced Computing and Simulations, Department of Physics & Astronomy, Department of Computer Science, Department of Material Science & Engineering, and Department of Biomedical Engineering, University of Southern California, Los Angeles, California 90089, USA*

[2]*Department of Physics, Kumamoto University, Kumamoto 860-8555, Japan*

[3]*Biological Computation and Visualization Center, Louisiana State University, Baton Rouge, Louisiana 70803, USA*

[4]*Studsvik Neutron Research Laboratory, University of Uppsala, Nyköping, Sweden*

The pressure-induced structural transformation in cadmium selenide is studied with the isothermal-isobaric molecular-dynamics method and electronic-structure calculations based on the density-functional theory. The reversible transformation between the fourfold-coordinated wurtzite structure and the sixfold-coordinated rocksalt structure is successfully reproduced in the molecular-dynamics simulations, in which atomistic transition mechanisms including the existence of a metastable state as well as barrier states along the transition paths are observed. Accurate density-functional calculations confirm these transition paths. It is shown that there are at least three transition paths, which are characterized by atomic shifts in the (0001) plane of the wurtzite structure. The energy barrier for the transformation is found to be about 0.13 eV/pair and is almost independent of the paths.

I. INTRODUCTION

The pressure-induced phase transformations from the fourfold- to the sixfold-coordinated structures in the semiconductor compounds have been extensively studied for the last few decades[1,2] for microscopic understanding as well as technological applications. The important point in considering the transformation mechanism is that the zinc-blende (ZB) or wurtzite (WZ) structure has to be transformed continuously into the rocksalt (RS) structure without any bond breaking in order that the transformation take place with reasonably lower-energy barrier. From this point of view, a mechanism has been proposed for the transformation from the ZB to RS structures.[3,4] The pathway and barrier state of the ZB-RS transformation are well understood as confirmed by the electronic-structure calculations based on density-functional theory[5] (DFT) as well as molecular-dynamics (MD) simulations.[3,6]

While the ZB-RS transformation is well established, the transformation mechanism from the WZ to RS structures is not well known so far despite many efforts.[7–12] Shock compression experiments by Sharma and Gupta[7] on CdS suggested that the basal planes of hexagon in the WZ structure are shifted alternately under pressure with a uniaxial strain perpendicular to both the a and c axes, and the system transforms into a metastable face-centered-orthorhombic (fco) structure, which is followed by a subsequent transformation to the RS structure. DFT calculations by Knudson *et al.*[8] showed that the metastable structure is not the fco but a face-centered-tetragonal (fct) structure. Recently, Limpijumnong and Lambrecht[9,10] proposed a homogeneous orthorhombic shear-strain deformation path for the WZ-RS transformation in GaN, which is slightly different from previous two mechanisms in the intermediate states. Al-

though they have given the detailed investigation of the energetics along the proposed transition path by DFT, there remain some questions as for the structure of metastable state and the possibility of other transformation paths.

One of the materials for which the WZ-RS transformation is of great interest is CdSe. CdSe is an important material for technological applications such as optical devices.[13] For nanocrystalline CdSe,[14,15] effects of the crystalline size of the WZ-RS transition pressure have been studied extensively, with the hope to stabilize new structures that are not stable in the bulk. Understanding the mechanism for the bulk WZ-RS transformation is imperative to understand and control the nanocrystalline transitions. While the WZ-RS transition pressure has been investigated experimentally[16,17] and theoretically,[18,19] no transformation mechanism has been proposed for bulk CdSe so far. In this paper, we investigate the mechanism of the WZ-RS transformation in CdSe using the electronic-structure calculations based on the DFT as well as the MD simulations. The DFT calculations are carried out for the atomic structures along the transition paths observed by the MD simulations to obtain the reliable results for the energy barrier and the structure of metastable state. We found that there are at least three structural transformation paths, which are characterized by atomic shifts in the (0001) plane of the WZ structure. Each mechanism has three equivalent directions and has unique strain.

II. METHOD OF CALCULATION

For the DFT calculations, we use the generalized gradient approximation[20] for the exchange-correlation energy. The ultrasoft pseudopotential[21] is employed for the interaction between the valence electrons and ions. The electronic wave functions are expanded by the plane-wave basis set with cut-
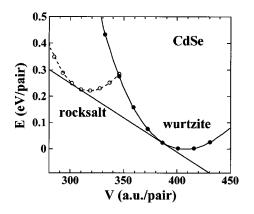
FIG. 1. Energy-volume relation for crystalline CdSe calculated by DFT. The solid circles correspond to the wurtzite structure, and the open circles correspond to the rocksalt structure. From these curves, the transition pressure is estimated to be about 2.5 GPa, being in agreement with the experiments (Refs. 16 and 17).

off energies for the wave functions and the charge density being 13 and 80 Ry, respectively. Figure 1 shows the energy-volume relation for the crystalline CdSe calculated by DFT. From a common-tangent construction the transition pressure is estimated to be 2.5 GPa, which is in good agreement with experimental values.[16,17] The lattice constants and the bulk modulus are also in accordance with the experimental[22,23] and other theoretical[18,19,24] values.

For the MD simulations, we use the interatomic potential scheme consisting of two- and three-body terms.[27,28] The two-body terms represent steric repulsion, Coulombic forces, charge-dipole, and van der Waals interactions. The three-body terms account for bond bending and stretching. In the present work, we use this scheme with the parameters optimized to reproduce a selected experimental data for CdSe. Our fitting database includes crystalline lattice constants, cohesive energies, elastic constants, melting temperature, and structural transition pressures.

We perform isothermal-isobaric MD simulations,[25,26] starting with $6\times6\times6$ orthorhombic unit cells (8 atoms/unit cell) of CdSe in the wurtzite structure. The thermostat and barostat time constants are chosen to be 205 and 2050 fs, respectively. A typical MD schedule is as follows: beginning with CdSe in the WZ structure at a temperature of 300 K and a pressure of 0.5 GPa, the pressure is raised in steps of 0.5 GPa at a rate of 1 GPa per 1000 time steps (1 time step is 2 fs). At each pressure the system is thermallized for 5000 time steps. This procedure is carried out until the desired maximum pressure is reached. Metastable and completely transformed structures are identified by plateaus in the variation of the atomic coordination as a function of time. Although the rate at which the pressure is increased is rather high and may affect the transformation pressure, the transformation paths observed in MD simulations are confirmed by the DFT calculations, and thus the conclusions of the paper are independent of the rate.

III. RESULTS AND DISCUSSIONS

We first explain simpler two structural transformation paths from the WZ to RS structures observed in our MD simulations, which are summarized in Fig. 2. We consider a WZ cell as an orthorhombic structure with lattice parameters a, b ($=\sqrt{3}a$), and c as shown in Fig. 2(a). One mechanism we have obtained is consistent with the previously proposed mechanisms,[7–12] which include the deformation of the orthorhombic structure accompanied with the transformation into the RS structure consisting of two mutually orthogonal strains. If the ratios b/a and c/a become equal to unity and the atomic positions are shifted appropriately, the WZ structure can be transformed into the RS structure as shown in Fig. 2(f). This RS structure is hereafter referred as RS-I. According to this transition mechanism, the crystallographic orientations of the WZ structure are related to those of the RS-I structure as $[10\bar{1}0]_{WZ}\|[100]_{RS\text{-}I}$, $[0100]_{WZ}\|[010]_{RS\text{-}I}$,
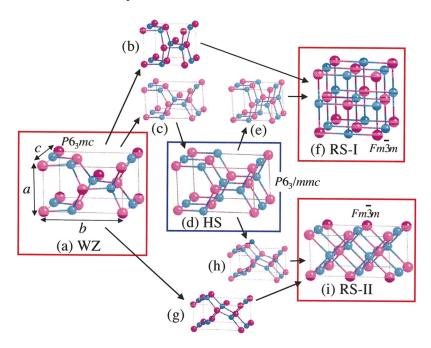

FIG. 2. (Color) Summary of the structural transformation from the wurtzite to the rocksalt structures in CdSe observed in our MD simulations. Each figure shows atomic configuration in the orthorhombic unit cell of CdSe. The magenta and blue spheres show the positions of Cd and Se atoms, respectively.

TABLE I. The ratios b/a and c/a of the lattice parameters and the atomic coordinates in the orthorhombic cells for the WZ, RS-I, RS-II, and HS structures. The orthorhombic lattice vectors are taken to be $\vec{a}_1=b\hat{x}$, $\vec{a}_2=a\hat{y}$, and $\vec{a}_3=c\hat{z}$.

	WZ $P6_3mc$	RS-I $Fm\,3m$	RS-II $Fm\,3m$	HS $P6_3/mmc$
b/a	$\sqrt{3}$	1	2	$\sqrt{3}$
c/a	1.63	1	$\sqrt{2}$	1.23
Cd (x,y,z)	(0,0,0)	(0,0,0)	(0,0,0)	(0,0,0)
	(1/2,1/2,0)	(1/2,1/2,0)	(1/2,1,0)	(1/2,1/2,0)
	(1/3,0,1/2)	(1/2,0,1/2)	(1/4,1/2,1/2)	(1/3,0,1/2)
	(5/6,1/2,1/2)	(1,1/2,1/2)	(3/4,1/2,1/2)	(5/6,1/2,1/2)
Se (x,y,z)	(0,0,3/8)	(0,0,1/2)	(0,0,1/2)	(0,0,1/2)
	(1/2,1/2,3/8)	(1/2,1/2,1/2)	(1/2,1,1/2)	(1/2,1/2,1/2)
	(1/3,0,7/8)	(1/2,0,1)	(1/4,1/2,1)	(1/3,0,1)
	(5/6,1/2,7/8)	1,1/2,1	(3/4,1/2,1)	(5/6,1/2,1)

and $[0001]_{WZ}\|[001]_{RS-I}$. The internal coordinates of atoms as well as the ratios b/a and c/a of the orthorhombic cells of the WZ and RS-I structures are listed in Table I.

Another way of deformation of the orthorhombic structure with two mutually orthogonal strains to transform the WZ to the RS structures corresponds to another transition path observed in our MD simulations. In this mechanism, atoms in the $(10\bar{1}0)$ plane in the WZ structure shift their positions along the [0100] direction, and b/a and c/a become 2 and $\sqrt{2}$, respectively. The final RS structure, hereafter referred as RS-II, is shown in Fig. 2(i). The crystallographic orientations in the WZ and RS-II structures are related as $[10\bar{1}0]_{WZ}\|[110]_{RS-II}$, $[0100]_{WZ}\|[\bar{1}10]_{RS-II}$, and $[0001]_{WZ}\|[001]_{RS-II}$. The internal coordinates of atoms as well as the ratios b/a and c/a of the orthorhombic cell of the RS-II structures are also listed in Table I.

To study the energetics of these transition paths accurately, we have minimized the enthalpy using DFT at a given pressure with respect to the orthorhombic lattice vectors at a given atomic configuration along a chosen path. We have investigated the path from WZ to RS-I and that from WZ to RS-II by linearly interpolating the atomic coordinates in these structures. The coordinates of ith atom in a intervening structure between WZ and two RS phases are given by $\vec{r}_i = (1-\eta)\vec{r}_{WZ,i} + \eta\vec{r}_{RS,i}(0 \leq \eta \leq 1)$, where $\vec{r}_{WZ,i}$ and $\vec{r}_{RS,i}$ are the atomic coordinates in the WZ and RS structures, respectively (see Table I), and the enthalpy is minimized for each η. Note that such defined path from WZ to RS-I is equivalent to that proposed for GaN in Ref. 9. The yellow-open and red-solid circles in Fig. 3 show the enthalpy change along the paths from WZ to RS-I and from WZ to RS-II, respectively, calculated at the pressure of 2.5 GPa, which is the WZ-RS transition pressure. It is found that the energy barrier for the path from WZ to RS-II is lower than that from WZ to RS-I and that there is no metastable structure along these paths. The barrier states occur at $x=0.5$ and 0.563 for the paths from WZ to RS-I and from WZ to RS-II, respectively, as shown in Figs. 2(b) and 2(g).

In our MD simulations, a fivefold-coordinated structure has been observed as a transition state during the transforma-

tion from the WZ to the RS structure. As shown in Fig. 2(d), their intermediate structure consists of stacked flat honeycomb lattices in the c direction, which we refer as HS. Note that the DFT calculations[9] have shown that the same intermediate phase exists in MgO, which, however, has no stable WZ structure. The symmetry is represented by space group $P6_3/mmc$, and the atomic coordinates and lattice parameters (b/a and c/a) are listed in Table I. The transformation from WZ to HS is straightforward in the sense that the hexagonal basal planes of cation and anion in the WZ structure are shifted alternatively along the c axis to form a flat plane. Also, the enthalpy of the HS phase in CdSe is calculated by DFT to be about 0.1 eV/pair measured from the WZ phase, which is lower than the energy barriers for the transition paths linearly interpolating the atomic coordinates in WZ and RS as shown in Fig. 3. We have thus investigated the transition from WZ to RS with the DFT in two parts: from WZ to HS and from HS to RS. To discuss these transformations with the linearly interpolated transition paths, we specify WZ and RS as $\eta=0$ and 1, respectively, and the HS structure is specified as $\eta=0.5$. The coordinates in a intervening structure are defined as $\vec{r}_i = (1-2\eta)\vec{r}_{WZ,i} + 2\eta\vec{r}_{HS,i}$ for $0 \leq \eta \leq 0.5$ between the WZ and HS phases and $\vec{r}_i = 2(1-\eta)\vec{r}_{HS,i} + (2\eta-1)\vec{r}_{RS,i}$ for $0.5 \leq \eta \leq 1$ between the HS and RS phases, where $\vec{r}_{HS,i}$ are the atomic coordinates in the HS structure. The red-solid triangles plotted for $0 \leq \eta \leq 0.5$ in Fig. 3 display the enthalpy change along the path from WZ to HS. The barrier state occurs at around $\eta=0.35$ and is shown in Fig. 2(c). The yellow-open and red-solid triangles plotted for $0.5 \leq \eta \leq 1$ in Fig. 3 show the enthalpy change along the paths from HS to RS-I and from HS to RS-II, respectively. We see that the energy barriers for these paths are lower than those for the paths linearly interpolating the WZ and RS structures shown by the circles, while they are higher than that between WZ and HS. These barrier states are displayed in Figs. 2(e) and 2(h). It is found that the HS phase appears as a metastable state, which suggests that the system may be trapped in this structure as was observed in our MD simulations. Since the energy barrier for the path from HS to RS-II is lower than that from HS to RS-I, it is concluded that the most favorable path is from WZ to RS-II through the HS
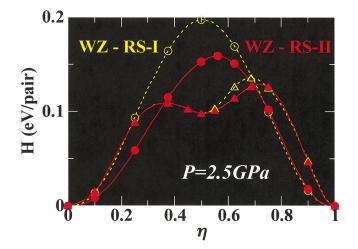
FIG. 4. Enthalpy as a function of pressure along the transition path from WZ ($\eta=0$) to RS-II ($\eta=1$) through HS ($\eta=0.5$).

FIG. 3. (Color) Enthalpy as a function of atomic configuration η. The wurtzite (WZ) and rocksalt (RS) structures correspond to $\eta=0$ and 1, respectively. The yellow-open and red-solid symbols show the enthalpy changes calculated along the transformation paths from WZ to RS-I and from WZ to RS-II, respectively. The circles correspond to the paths linearly interpolating the atomic coordinates in the WZ and RS structures. For the lines shown by triangles, the enthalpy of the honeycomb-stacked (HS) structure is shown by $\eta=0.5$.

structure. We however note that both paths from WZ to RS may take place in real materials because the difference in the energy barriers is rather small, ~ 0.01 eV/pair.

Figure 4 shows the enthalpy change as a function of pressure for the path from WZ to RS-II through HS. With increasing the pressure, the RS phase becomes more stable. It is found that the barrier state is at around $\eta=0.8$ between HS and RS-II when the pressure is less than 3, while it occurs at around $\eta=0.3$ between WZ and HS for higher pressures. It is also found that the HS state is metastable for the pressures less than four.
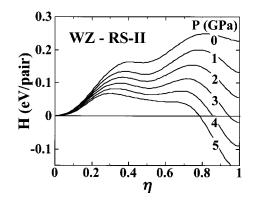
Next, we discuss another transition mechanism from WZ to RS found in our MD simulations, which involves a shear deformation of unit cells in the (0001) plane (the *a-b* plane) of the WZ phase with compression in the *c* direction. This transformation takes place with nine orthorhombic cells in the WZ structure. The RS structure obtained through this mechanism has different crystallographic orientations from those in RS-I and RS-II, and is referred to as RS-III. As stated above, the two structural transformation paths from WZ to RS-I and from WZ to RS-II are characterized by atomic shifts in the *a-b* plane of the WZ structure. Figures 5 and 6 show the changes of atomic configuration in the *a-b* plane for the transition from WZ to RS-I and from WZ to RS-II, respectively. The small arrows drawn in the WZ structures show the directions to which the internal atomic coordinates are shifted. The transformation from WZ to RS-I is characterized by the atomic shift to the $[10\bar{1}0]$ direction as shown in Fig. 5, while the atomic shifts to the $[0100]$ direction take place in the transformation from WZ to RS-II as shown in Fig. 6. The mechanism of the transformation from
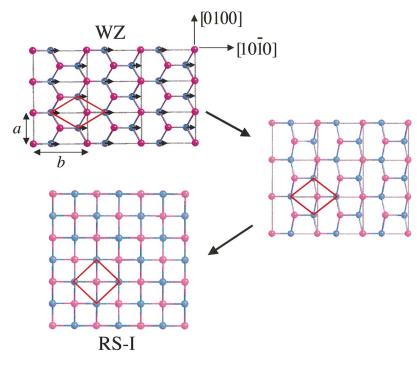

FIG. 5. (Color) The mechanism of the structural transformation from WZ to RS-I. The magneta and blue spheres show the positions of Cd and Se atoms, respectively. The small arrows in the WZ structure show the directions to which the internal atomic coordinates are shifted.
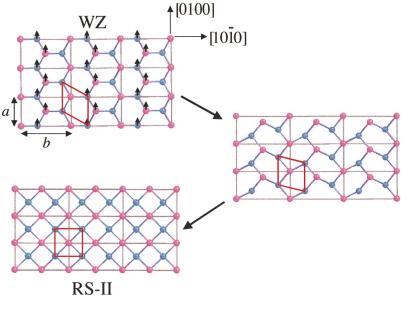
FIG. 6. (Color) The mechanism of the structural transformation from WZ to RS-II. The magneta and blue spheres show the positions of Cd and Se atoms, respectively. The small arrows in the WZ structure show the directions to which the internal atomic coordinates are shifted.

WZ to RS-III is displayed in Fig. 7. In this transformation, the atoms on the $(1\bar{1}00)$ plane of the WZ structure move their positions alternatively along the [0010] direction; the positions of atoms on the $(1\bar{1}00)$ planes denoted by $(2,2')$ and $(3,3')$ in Fig. 7 are shifted to the [0010] and $[00\bar{1}0]$ directions, respectively, while those on the planes denoted by $(1,1')$ are unchanged along this direction. Accompanied with these shifts of the atomic positions, the $(1\bar{1}00)$ planes are shifted along the $[1\bar{1}00]$ direction to become equidistant between the planes in the RS phase. The crystallographic orientations in the WZ and RS-III structures are related as $[0010]_{WZ} \| [110]_{RS\text{-}III}$ and $[0001]_{WZ} \| [001]_{RS\text{-}III}$. The energy barrier calculated by DFT for this transformation is about 0.13 eV/pair, which is as high as those for transitions from WZ to RS-I and from WZ to RS-II.

DFT calculations by Knudson *et al.*[8] suggested that the fct structure is metastable in CdS. To transform the structure

from WZ to fct, atoms in the basal planes at $c/2$ and $7c/8$ shift along the b axis so that their x coordinates become 0.5 [see Fig. 2(a)]. Our DFT estimate of the energy barrier of this transition is as high as 0.18 eV/pair, and we found that the fct phase is neither the metastable nor the barrier states in the case of CdSe.

IV. SUMMARY

We have proposed atomistic mechanisms for the structural transformation from the wurtzite to rocksalt phases in CdSe based on the observations in our MD simulations. The main difference between these mechanisms lies in the ways atomic positions shift parallel to the (0001) plane in the WZ structure. One mechanism involves shifts of the atomic positions along the [1000] direction, while the other along the $[10\bar{1}0]$ direction. We note that these mechanisms have three
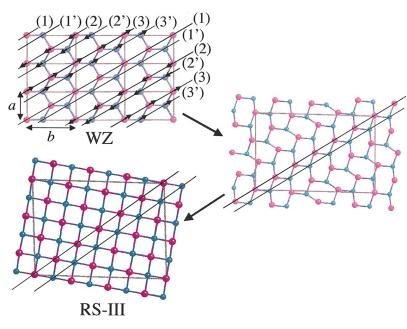

FIG. 7. (Color) The mechanism of the structural transformation from WZ to RS-III. The magneta and blue spheres show the positions of Cd and Se atoms, respectively. The small arrows in the WZ structure show the directions to which the internal atomic coordinates are shifted.

equivalent directions and that each transformation has a unique strain. We have also found another mechanism of the transition from WZ to RS, which takes place with nine orthorhombic cells in the WZ structure. It has been confirmed from the DFT calculations that the energy barrier for the transformation is about 0.13 eV/pair and is almost independent of the paths, which implies that any of these mechanisms occur in real materials.

[1] S. Froyen and M. L. Cohen, Phys. Rev. B **28**, 3258 (1983).

[2] R. Martonak, C. Molteni, and M. Parrinello, Phys. Rev. Lett. **84**, 682 (2000).

[3] F. Shimojo, I. Ebbsjo, R. K. Kalia, A. Nakano, J. P. Rino, and P. Vashishta, Phys. Rev. Lett. **84**, 3338 (2000).

[4] H. Sowa, Z. Kristallogr. **215**, 335 (2000).

[5] M. Catti, Phys. Rev. Lett. **87**, 035504 (2001).

[6] M. Wilson, F. Hutchinson, and P. A. Madden, Phys. Rev. B **65**, 094109 (2002).

[7] S. M. Sharma and Y. M. Gupta, Phys. Rev. B **58**, 5964 (1998).

[8] M. D. Knudson, Y. M. Gupta, and A. B. Kunz, Phys. Rev. B **59**, 11704 (1999).

[9] S. Limpijumnong and W. R. L. Lambrecht, Phys. Rev. Lett. **86**, 91 (2001).

[10] S. Limpijumnong and W. R. L. Lambrecht, Phys. Rev. B **63**, 104103 (2001).

[11] H. Sowa, Acta Crystallogr., Sect. A: Found. Crystallogr. **57**, 176 (2001).

[12] M. Wilson and P. A. Madden, J. Phys.: Condens. Matter **14**, 4629 (2002).

[13] C. B. Murray, C. R. Kagan, and M. G. Bawendi, Annu. Rev. Mater. Sci. **30**, 545 (2000).

[14] S. H. Tolbert and A. P. Alivisatos, J. Chem. Phys. **102**, 4642 (1995).

[15] J. N. Wickham, A. B. Herhold, and A. P. Alivisatos, Phys. Rev. Lett. **84**, 923 (2000).

[16] A. L. Edward and H. G. Drickamer, Phys. Rev. **122**, 1149 (1961).

[17] A. Jayaraman, W. Klement, Jr., and G. C. Kennedy, Phys. Rev. **130**, 2277 (1963).

[18] O. Zakharov, A. Rubio, and M. L. Cohen, Phys. Rev. B **51**, 4926 (1995).

[19] M. Côté, O. Zakharov, A. Rubio, and M. L. Cohen, Phys. Rev. B **55**, 13025 (1997).

[20] J. P. Perdew, K. Burke, and M. Ernzerhof, Phys. Rev. Lett. **77**, 3865 (1996).

[21] D. Vanderbilt, Phys. Rev. B **41**, 7892 (1990).

[22] *Handbook of Chemistry and Physics*, edited by D. R. Lide (CRC Press, New York, 2001).

[23] *Landolt-Bornstein: Numerical Data and Functional Relationships in Science and Technology*, edited by O. Madelung, M. Schulz, and H. Weiss (Springer-Verlag, Berlin, 1982), Vol. 17b.

[24] S. Wei and S. B. Zhang, Phys. Rev. B **62**, 6944 (2000).

[25] G.J. Martyna, D.J. Tobias, and M.L. Klein, J. Chem. Phys. **101**, 4177 (1994).

[26] M. Tuckerman, B.J. Berne, and G.J. Martyna, J. Chem. Phys. **97**, 1990 (1992).

[27] P. Vashishta *et al.*, in *Amorphous Insulators and Semiconductors*, edited by M. F. Thorpe and M. I. Mitkova (Kluwer, Dordrecht, 1996), p. 151.

[28] J. P. Rino, I. Ebbsjö, P. S. Branicio, R. K. Kalia, A. Nakano, and P. Vashishta, Phys. Rev. B **70**, 045207 (2004).